genesis 29:163–171 (2001)

LETTER

The Winged Helix/Forkhead Transcription Factor *Foxq1* Regulates Differentiation of Hair in Satin Mice

Hee-Kyung Hong,[1,†], Janice K. Noveroske[2], Denis J. Headon[3], Tong Liu[4], Man-Sun Sy[4], Monica J. Justice[2], and Aravinda Chakravarti[1*]

[1]Department of Genetics and Center for Human Genetics, Case Western Reserve University and University Hospitals of Cleveland, Cleveland, Ohio
[2]Department of Molecular and Human Genetics, Baylor College of Medicine, Houston, Texas
[3]Department of Cell Biology, Baylor College of Medicine, Houston, Texas
[4]Department of Pathology, Case Western Reserve University and University Hospitals of Cleveland, Cleveland, Ohio

Received 4 January 2000; Accepted 7 February 2001

Summary: Satin (*sa*) homozygous mice have a silky coat with high sheen arising from structurally abnormal medulla cells and defects in differentiation of the hair shaft. We demonstrate that the winged helix/forkhead transcription factor, *Foxq1* (Forkhead box, subclass *q,* member *1*) is mutant in *sa* mice. An intragenic deletion was identified in the radiation-induced satin mutant of the SB/Le inbred strain; a second allele, identified by an *N*-ethyl-*N*-nitrosourea (ENU) mutagenesis screen, has a missense mutation in the conserved winged helix DNA-binding domain. Homozygous mutants of the two alleles are indistinguishable. We show that *Foxq1* is expressed during embryogenesis and exhibits a tissue-restricted expression pattern in adult tissues. The hair defects appear to be restricted to the inner structures of the hair; consequently, *Foxq1* has a unique and distinct function involved in differentiation and development of the hair shaft. Despite an otherwise healthy appearance, satin mice have been reported to exhibit suppressed NK-cell function and alloimmune cytotoxic T-cell function. We show instead that the immune defects are attributable to genetic background differences. genesis 29:163–171, 2001. © 2001 Wiley-Liss, Inc.

Key words: Foxq1; winged helix/forkhead transcription factor; satin; hair differentiation

The development of hair first involves the formation of epidermal placodes, the clumps of epithelial cells in lower layers of the epidermis that induce the condensation of specialized mesenchymal cells, dermal papilla. These cells are the source of complex inductive signals required for epidermal invagination and formation of epithelial portion of the hair follicle. The epithelial cells adjacent to dermal papilla, also known as the hair matrix, are later stimulated and differentiated into mature hair structures (Hardy, 1992).

Once established, hair is produced by a cycle of tissue growth, degeneration, and renewal, defined by the three phases of anagen (the growth stage), catagen (the regression stage), and telogen (the stage of hair follicle quiescence). A number of mouse mutations, causing a wide spectrum of hair defects, have led to the identification of some of the molecular collaborators in hair follicle development and in its cyclic pattern of differentiation, including fibroblast growth factors (FGFs), bone morphogenetic proteins (BMPs), Sonic hedgehog (Shh), β-catenin, and proteins of the Notch signaling system (Oro and Scott, 1998; van Steensel *et al.*, 2000). We report here that a distinct recessive mutation satin (*sa*) in the winged helix (WH)/forkhead transcription factor affects the later stages of hair development, resulting in abnormal hair texture.

The satin (*sa*) mutation originally arose by gamma irradiation and in homozygous mice gives a silky appearance with a high sheen coat (Fig. 1) (Major, 1955). Histology and ultrastructure studies of plucked hairs reveal that all four types of pelage hair are present but that they are thinner than those in a normal hair shaft because the medullary cells contain far more fibrous material and, it is suggested, the satin hairs do not keratinize properly although the hair follicles are relatively normal in appearance (Trigg, 1972). We demonstrate an intragenic deletion in the coding region of the mouse *Foxq1* gene in the original satin allele and a missense mutation in a second satin allele identified by an *N*-ethyl-*N*-nitrosourea (ENU) mutagenesis screen. *Foxq1* (Forkhead box, subclass *q,* member *1,* formally known as *Hfh1*; Kaestner *et al.*, 2000) is a member of the evolutionarily conserved winged helix (WH)/forkhead tran-

Contract grant sponsor: NIH, grant number: HD 34857 (A.C.). Grant sponsor: Willson Foundation (to the Center for Human Genetics).

* Correspondence to: Aravinda Chakravarti, PhD, McKusick-Nathans Institute for Genetic Medicine, Jefferson Street Bldg, 2-109, Johns Hopkins University School of Medicine, Baltimore, MD 21287.
E-mail: aravinda@jhmi.edu

†Current address: Dept. of Neurobiology and Physiology, 2-160 Hogan Hall, Northwestern University, 2153 N. Campus Dr., Evanston, IL 60208.

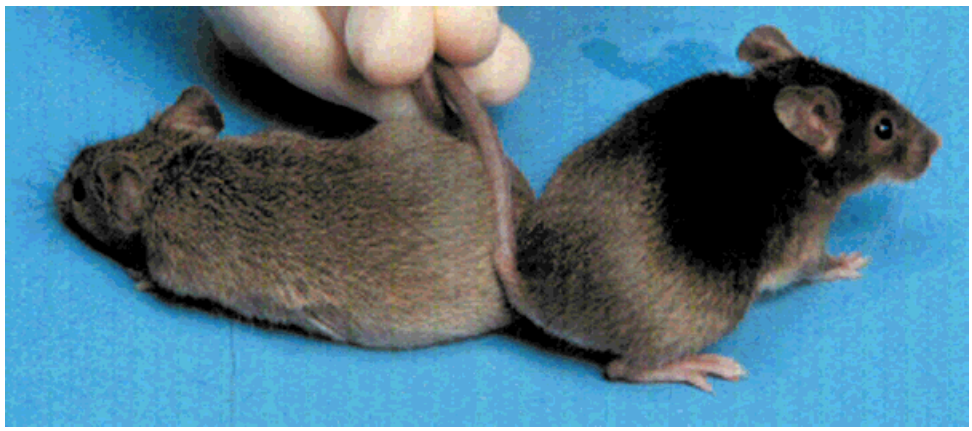

FIG. 1. The sa^{e1}/sa^{e1} mutant (right) adjacent to a control littermate (left) demonstrates the characteristic silky coat with high sheen.

scription factor gene family. Consequently, the phenotype in *sa/sa* mice must arise from the failure to activate or repress a downstream signal required for keratinization. Interestingly, satin mice have been reported to exhibit suppressed NK-cell function and alloimmune cytotoxic T-cell function, a phenotype exacerbated by the effects of the closely linked beige (*bg*) gene product (McGarry *et al*., 1984). This hair/T-cell function may not be a chance association; a number of other mouse mutations that affect hair development also exhibit abnormal immune systems (Sundbert and King, 1996). Significantly, the similar but more severe athymic and hair loss mutation nude (*nu*) is also mutant in the related WH/forkhead transcription factor *Foxn1* (Nehls *et al*., 1994).

The satin locus genetically maps to proximal mouse chromosome 13, between the markers D13Mit206 and D13Mit294 (Perou *et al*., 1997). We have previously cloned and mapped to this identical location a new member of the WH/forkhead transcription factor gene family, *Foxq1* (Hong *et al*., 1999). By virtue of the similarities between the nude and satin mutations, we explored *Foxq1* as a candidate gene for satin. We cloned the full-length mouse *Foxq1* gene by PCR amplification from mouse genomic DNA from strain 129 and a mouse yeast artificial chromosome (YAC) (Hong et al., 1999) using the rat *Foxq1* cDNA sequence (Clevidence *et al.*, 1993). Our sequence analyses reveal that both the rat and mouse *Foxq1* proteins are 400 residues and are encoded by a 1,200 bp intronless gene. The mouse and rat *Foxq1* have 93% nucleotide and 94% protein sequence identity, demonstrating that we have identified the orthologs (Fig. 2a). To further explore sequence conservation of *Foxq1*, we isolated the human ortholog (see Methods). Human *FOXQ1* consists of a 1,206 bp open reading frame encoding a transcript of 402 residues with an amino acid sequence identity of 79% to the mouse protein. The highest similarity between rat, mouse and human *Foxq1* is within the WH DNA-binding domain, which does not differ in amino acid sequence and shares 96% nucleotide sequence identity. In addition to the WH domain, the human, mouse, and rat proteins share marked amino acid sequence identity in several additional regions (Fig. 2a) that are often recognized in transcription factors (Mitchell and Tjian, 1989). These conserved segments include regions that are rich in acidic and serine residues (region I) at the NH_2-terminus and domains that are rich in serine residues (region II), proline residues (region III), and a distal conserved segment of 35 amino acids (region IV). Whether these evolutionarily conserved regions are required for transcription activation or repression is unknown.

In order to understand the nature of the phenotypic effects of satin, we explored the temporal and spatial expression pattern of *Foxq1*. We used Northern blot analysis of polyadenylated RNA prepared from adult tissues of wild-type mice and revealed a single $\approx$ 3kb band in all tissues examined (Fig. 2b). *Foxq1* was showed abundant expression in liver, moderately expression in kidney, and low expression in lung, brain, and testis; no detectable activity was observed in heart or spleen. These results are in contrast to the expression pattern observed in the rat, where *Foxq1* is moderately expressed in the lung and kidney of the adult but not in the liver, brain, or testis (Clevidence *et al*., 1993, 1994). These mouse-rat tissue-specific expression differences may be related to intrinsic functional differences of *Foxq1* in different species and require resolution by in situ hybridization analysis and studies of cellular distribution. Whether they are true orthologs are in question because the genes are not expressed in the same tissues. Nevertheless, the tissue-restricted expression pattern of *Foxq1* in adults suggests that *Foxq1* transcription is required for the maintenance of the differentiated phenotype. The *Foxq1* gene, in analogy to other related members, is likely to play crucial roles during embryogenesis. Thus, we investigated *Foxq1* expression at various stages of mouse development (Fig. 2c) and show that *Foxq1* is expressed throughout embryonic development. Phenotypic analysis does not suggest an embryonic phenotype and thus its role during embryogenesis remains unclear.

We searched for *Foxq1* gene mutations in satin on a beige background (SB/Le-*bg sa* / *bg sa*), in comparison to the wild-type (SB/Le-++/++). The SB/Le strain is

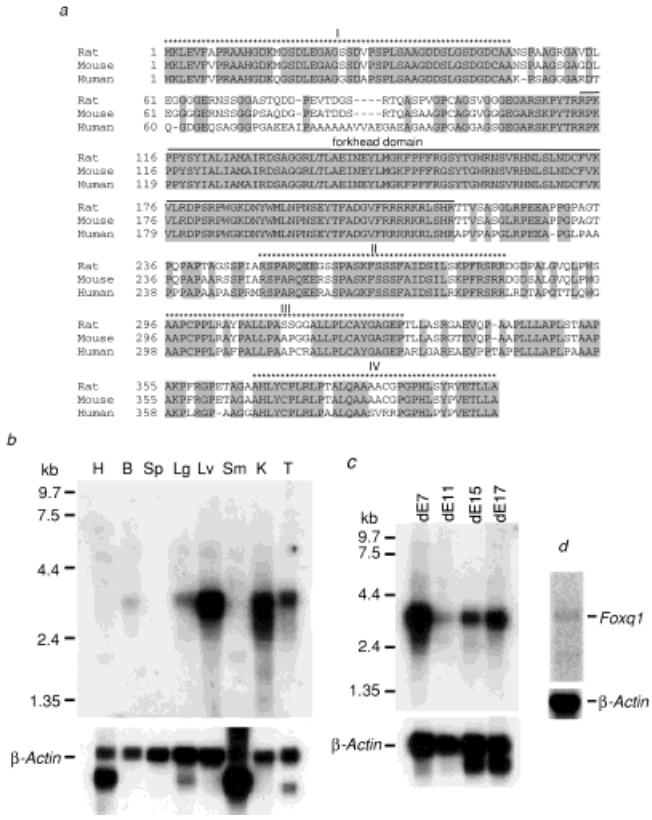

FIG. 2. (**a**) Amino acid sequences of rat, mouse, and human FOXQ1. Identical residues are shaded and the forkhead domain (winged helix motif) is designated by a line above the sequence. Asterisks above the sequence delineate four conserved regions indicating putative transcription activation and other functional domains. Nucleotide sequence analysis of the mouse *Foxq1* coding region and the published rat *Foxq1* cDNA showed a DNA sequence identity of 96% but a predicted protein sequence identity of only 63%. This discrepancy was resolved by resequencing the rat *Foxq1* gene and demonstrating multiple sequencing errors in the published rat *Foxq1* cDNA sequence (Clevidence *et al.*, 1993). The corrected protein sequence alignment of mouse and rat *Foxq1*, across known motifs, is shown and demonstrates an amino acid sequence identity of 94%. Amino acid sequence identity between the mouse and human proteins is 79%. A search of sequence databases showed that the mouse *Foxq1* gene is 99.4% identical in nucleotide sequence, and differs by three amino acids from the mouse HNF-3/fork head homologue-1 like gene (*Hfh-1L*; Frank and Zoll, 1998), which also maps to the same region of mouse chromosome 13. A comparison of the flanking genomic sequences of both genes indicates that *Foxq1* and *Hfh-1L* are identical. WH = winged helix domain; I = acidic and serine-rich domain; II = serine-rich domain; III = proline-rich domain; IV = functional conserved region. (**b**) Expression analysis of the mouse *Foxq1* gene. Northern blot analysis of various adult tissues shows an ≈ 3 kb *Foxq1* transcript in the liver and kidney, but weakly expressed in brain, lung and testis. (**c**) Expression analysis during mouse development shows high expression as early as dE7 but moderate expression subsequently (dE11, dE15, and dE17). Northern blots of 2 μg poly(A)$^+$ RNA from various mouse adult tisssues and embryonic stages (Clontech) were hybridized with a 706 nt probe corresponding to the 3′ end of the gene that lacks the WH DNA binding domain region (see Methods). Identical expression patterns were observed when hybridizing a probe that corresponds to the 5′ end of the gene. Molecular size standards (in kb) are shown to the left. B = brain; H = heart; Lg = lung; Lv = liver; Sm = skeletal muscle; Sp = spleen; K = kidney; T = testis. (**d**) Foxq1 expression in adult thymus from wild-type progenitor C3H mice.

derived from intercrosses of a stock carrying *bg* and *sa* alleles, both arising at the Oak Ridge National Laboratory in offspring from (101/Rl × C3H/Rl)F_1 mutagenized males (Oak Ridge, TN; Perou *et al.*, 1997). Consequently, we also analyzed *Foxq1* in the 101 and C3H strains. The mouse *bg* mutation maps proximal to *sa* on MMU13 and occurs within the *Lyst* gene, the human ortholog of which is mutant in Chediak-Higashi syndrome (Spritz, 1998). We performed polymerase chain reaction (PCR) amplification of the entire *Foxq1* coding region to reveal a deletion in homozygous satin mutants, as compared to wild-type SB/Le, 101 and C3H mice (Fig. 3a). Nucleotide sequencing demonstrated an intragenic 67 base-pair deletion (positions 686–752: numbered from the translation initiation site) and further base substitutions at positions 766 and 767 restricted to satin mutants (Fig. 3b). The deletion does not affect the first 228 residues, including the characteristic WH DNA-binding domain; however, it causes a frame shift resulting in a truncated 376 residue protein (Fig. 3c). Functional studies of the related WH/forkhead members *Foxa2* (*HNF-3β*) and *Foxn1* (*nu*) have shown that the conserved C-terminal regions are required for transcriptional activation of target genes (Qian and Costa, 1995; Schüddekopf, 1996). Consequently, we predict that the mutant satin protein will bind to its DNA targets but fail at transcriptional activation or repression because the specific C-terminal domains are missing.

To garner further evidence that *Foxq1* is mutant in satin we sought additional alleles from a screen using the mutagen *N*-ethyl-*N*-nitrosourea (ENU), known primarily to induce point mutations (Rinchik, 1991). A second mutant allele of *sa* was identified from a screen based on hair phenotype of offspring from matings between homozygous satin SB/Le females with mutagenized wild-type (101/Rl x CH3/Rl)F_1 males. This new *sa* mutant is predicted to be a compound heterozygote for the previously described intragenic deletion and a novel ENU-induced mutation. We cloned the products of PCR amplification of *Foxq1* from genomic DNA of sa^{e1} and showed by nucleotide sequencing of multiple clones that the shorter fragments contained the known 67 bp deletion but that the normal sized fragments harbored a T → G transversion at position 383 (numbered from the translation initiation site). This transversion mutation was not present in any of the parental genomes, 101 and C3H strains, or in the SB/Le - ++/++ wild-type and homozygous SB/Le - *bg sa/bg sa* mutant mice (Fig. 3d). This second mutation leads to the substitution of a hydrophobic isoleucine (Ile) residue by a polar serine (Ser) residue at position 128 (Ile128Ser) located in the WH domain (Fig. 3d). The isoleucine residue at amino acid 128 is predicted to lie in the first helix of the DNA-binding domain and is largely buried in the hydrophobic core of the polypeptide (Clark *et al.*, 1993). Significantly, Ile is a highly conserved residue at position 128 among all WH/forkhead family members examined in species ranging from yeast to human; the only evolutionary changes allowed have been to the hydrophobic methio-

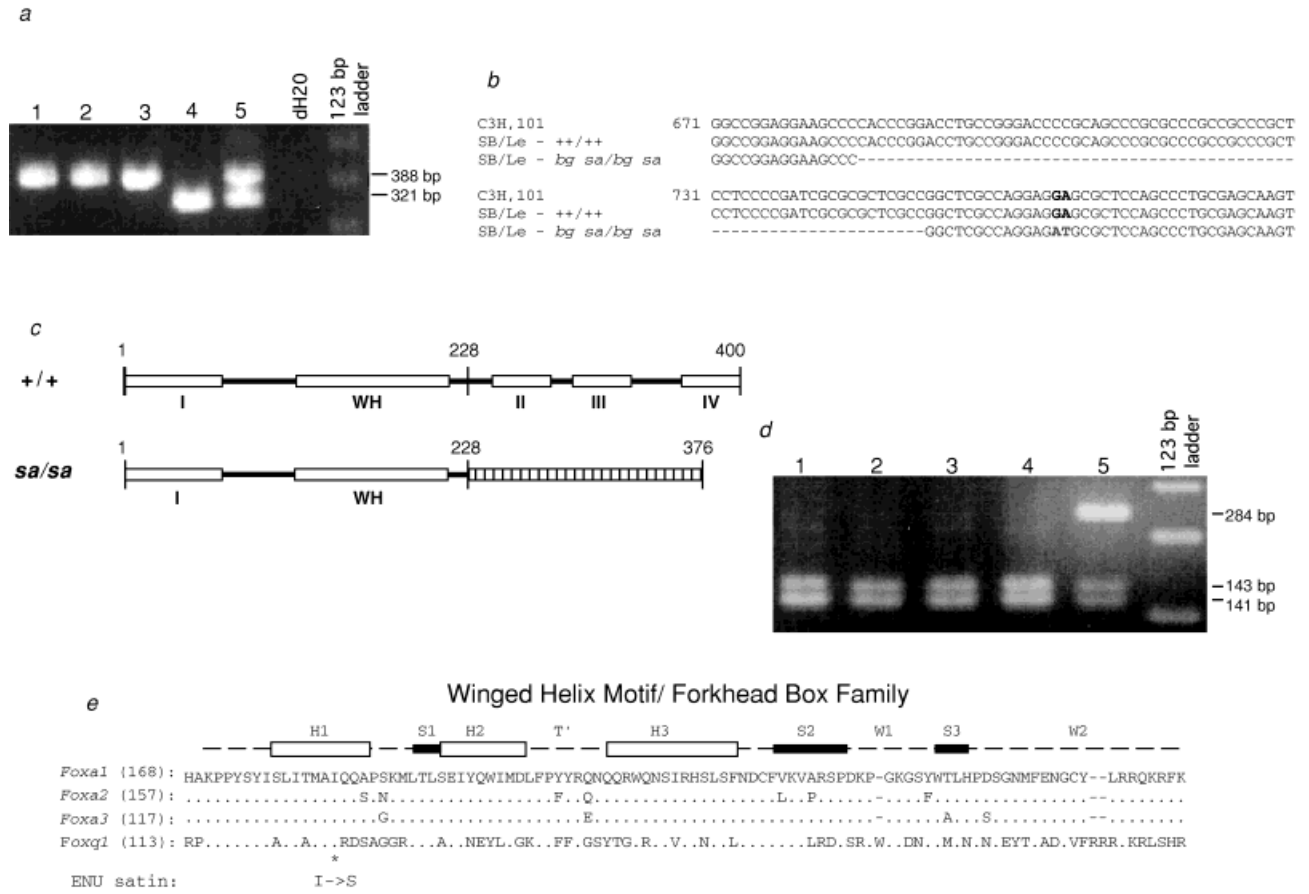

FIG. 3. (**a**) Radiation-induced *sa* allele has a mutation in *Foxq1*. PCR amplification of the *Foxq1* gene in C3H (lane 1), 101 (lane 2), wild-type SB/Le (SB/Le - ++/++; lane 3), radiation-induced satin (SB/Le-*bg sa/bg sa*; lane 4), and ENU-induced satin in a compound sa^{e1}/sa heterozygote (lane 5; see text) using primers m*Foxq1*.F2 and m*Foxq1*.R5. Only the satin mutants (lanes 4 and 5) show a smaller PCR fragment indicating an intragenic deletion. (**b**) The 67 bp deletion at bp 686–752 and two nucleotide substitutions at bp 766 and 767 were detected in the radiation-induced satin mutant by sequence analysis; nucleotides are numbered from the translation initiation site. (**c**) Predicted structures of wild-type and mutant *Foxq1* protein. The mutant protein is predicted to retain the first 228 amino acids, including the WH DNA binding domain, but a novel translated frame begins thereafter (indicated by ▥); deletion results in a shorter protein of 376 residues. WH = winged helix domain; I = acidic and serine-rich domain; II = serine-rich domain; III = proline-rich domain; IV = functional conserved region. (**d**) ENU-induced *sa* allele has a mutation in *Foxq1*. The new satin mutant is a compound heterozygote for the intragenic deletion (*sa*) and a novel ENU-induced point mutation (sa^{e1}). The radiation-induced intragenic deletion is detected by PCR analysis using primers m*Foxq1*.F2 and m*Foxq1*.R5 (Fig. 3a, lane 5). The T→G transversion is detected in the ENU-induced allele at bp 383 resulting in a Ile to Ser substitution at residue 128. This mutation is detected by PCR analysis using primers m*Foxq1*.F3 and m*Foxq1*.R4 and restriction enzyme digestion with *Fok*1. Electrophoresis resolves two fragments of 141 and 143 bp from the wild-type allele and 284 bp from the ENU-mutant allele. The compound heterozygote satin shows all three bands (lane 5). Note that the ENU-mutant allele is not present in the parental strains (C3H, lane 1; 101, lane 2; SB/Le - ++/++, lane 3; SB/Le - *bg sa/bg sa*; lane 4). (**e**) The mutation (*) is located at a highly conserved site in the first helix of the WH domain as compared to *Foxa1, Foxa2, Foxa3* (Clark *et al*., 1993). The common secondary structural elements are indicated: α- Helices (H1, H2, and H3); β-strand (S1, S2, and S3); winglike loops (W1 and W2); and the region between H2 and H3 (T′) (Kaufmann and Knochel, 1996).

nine or leucine residues (Kaufmann and Knochel, 1996). Finally, the N-terminus of the WH motif is the most conserved region in this protein family and has been proposed to act as a localization signal necessary for nuclear targeting (Qian and Costa, 1995). Therefore, we predict that the Ile128Ser mutation affects the three-dimensional structure of the protein and compromises or even prevents the binding of the WH domain to its targets, probably resulting in a loss-of-function allele. It is possible that the mutant protein has impaired nuclear targeting as well. Subsequent breeding experiments showed that homozygous Ile128Ser mutants (ss^{e1}/sa^{e1}; Fig. 1) and compound heterozgote mutants (sa^{e1}/sa) are visibly indistinguishable from the homozygous satin mice of the original radiation induced allele (*sa/sa*). Thus, both sa^{e1} and *sa* are equivalent recessive alleles.

In order to understand the satin phenotype, we compared the histology of *Foxq1*-expressing tissues from homozygous satin mice (sa^{e1}/sa^{e1}) and their wild-type and heterozygous littermates. There were no gross morphological differences in the kidney, liver, brain, and lung; therefore, *Foxq1* is apparently dispensable for de-

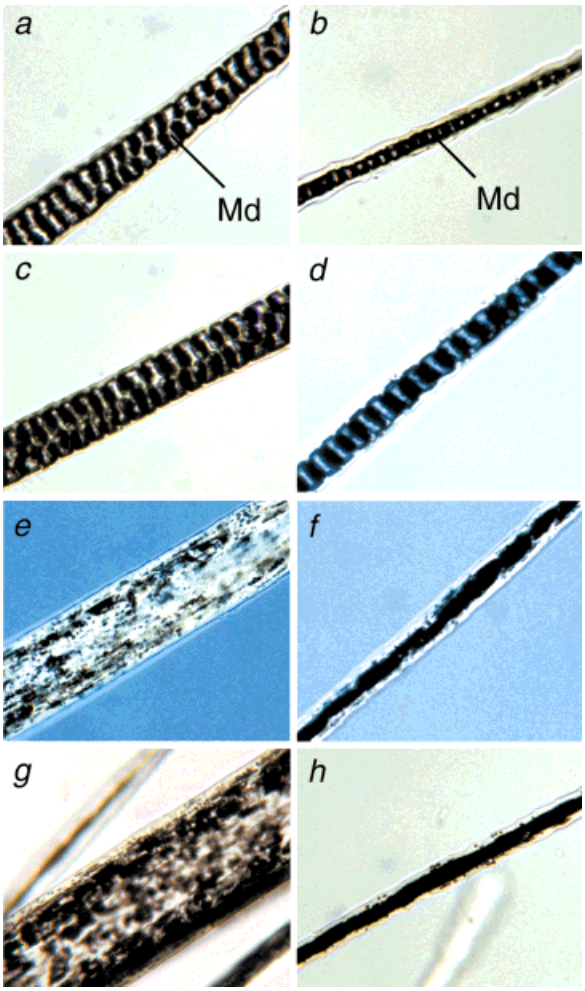

FIG. 4. Light microscopy (≈ 1500×) of pelage hair (a–h). Left and right panels show the inner structures of *awl* and *zigzag* hairs, respectively: (**a, b**) wild-type, +/+; (**c, d**) heterozygote, +/sa^{e1}; (**e, f**) ENU-induced satin, sa^{e1}/sa^{e1}; (**g,h**) radiation-induced satin, *sa/sa*. Md = medullary layer.

velopment or maintenance of the differentiated phenotype of these tissues. Next, we examined pelage hairs by scanning electron and light microscopy. The normal hair shaft is composed of cuticle, cortex, and medulla. The cuticle is made up of a series of thin, overlapping scales that point distally; the cortex, enveloped by the cuticle scales, forms a hardened hollow cylinder filled with bundles of filaments, and the medullary cells are arranged in regular rows and interlocked by the cortical cells (Parakkal, 1969). We did not detect any morphological differences on the surface of the hairs from mutants (data not shown). However, the inner structures of hair from satin mutants showed striking differences as compare to their wild-type and heterozygote littermates (Fig. 4a–h). The medullary cells consist of structural proteins, vacuoles, and pigment granules; fully differentiated cells contain large intracellular vacuoles that are later replaced with air spaces, giving a banding pattern in dry hair (Parakkal, 1969). In satin mice, the medullary cells are difficult to distinguish and lack air spaces and cortical ridges. In addition, satin hairs show clumping of melanin granules and lack the characteristic septation observed in normal mouse hairs. Under transmission electron microscopy (Fig. 5a, b), similar phenotypic changes were observed. Clearly, the medullary cells were disorganized throughout the hair shaft and the air spaces did not form. In addition, although not as apparent, there were some changes in the cortical cells. In general, the cortical cells were slightly thicker in the mutants as compare to the cells of the wild type. To determine if the hair phenotypes observed correlate with the expression of *Foxq1*, we examined wild-type skin from a postnatal day 9 mouse, when the hair shaft is in full growth (mid-anagen). The results of our in situ hybridization studies demonstrated that *Foxq1* is indeed expressed at high levels in the central cells (premedullary cells) above the dermal papilla that are in the process of differentiating into the hair shaft (Fig. 5c, d). *Foxq1* expression commences in approximately the middle of the follicle bulb and into the lower portion of the hair shaft. *Foxq1* is not detected in undifferentiated matrix cells, the lower portion of the bulb. Given the resolution of the in situ hybridization, it is possible that *Foxq1* is also expressed in cortical cells, however, the expression does not seem to be cuticular. Thus, the expression of *Foxq1* in hair follicles coincides with the hair phenotype in satin mice. Interestingly, preliminary histological analysis of adult back-skin sections failed to detect any marked difference in satin mutants as compared to their wild-type littermates (data not shown), indicating that *Foxq1* is unlikely to be involved in skin development and in the early steps of hair follicle formation.

Mutations with skin and hair abnormalities are important for elucidating the molecular mechanisms involved in the development and maintenance of these tissues (Sundberg and King, 1996). Another winged helix *Foxn1* gene is responsible for the nude (*nu*) mouse and rat phenotypes of hairlessness and congenital athymia (Nehls *et al.*, 1994). Similarly, in the human, a homozygous nonsense mutation in the *FOXN1* gene causes severe T-cell immunodeficiency, congenital alopecia, and nail dystrophy (MIM database no. 601705) (Frank *et al.*, 1999). Analogous to the hair and immune phenotype in nude mice, a prior study has observed suppressed NK and CT immune cell function in homozygous satin mice (*sa/sa*); the phenotype is more severe in double homozygotes with beige (McGarry *et al.*, 1994), suggesting cooperative interaction of *Foxq1* and *LYST*. Indeed, the *Foxq1* transcript is normally expressed in adult thymus in wild-type progenitor C3H mice (Fig. 2d). Although the satin phenotype is not as severe as nude (*nu*), satin mutants could provide important mouse models for the identification of additional components in the development and maintenance of the normal immunological function in mammals. We used contemporary methods to characterize the specific nature of immune defects in satin mice by examining their lymphocyte subpopula-

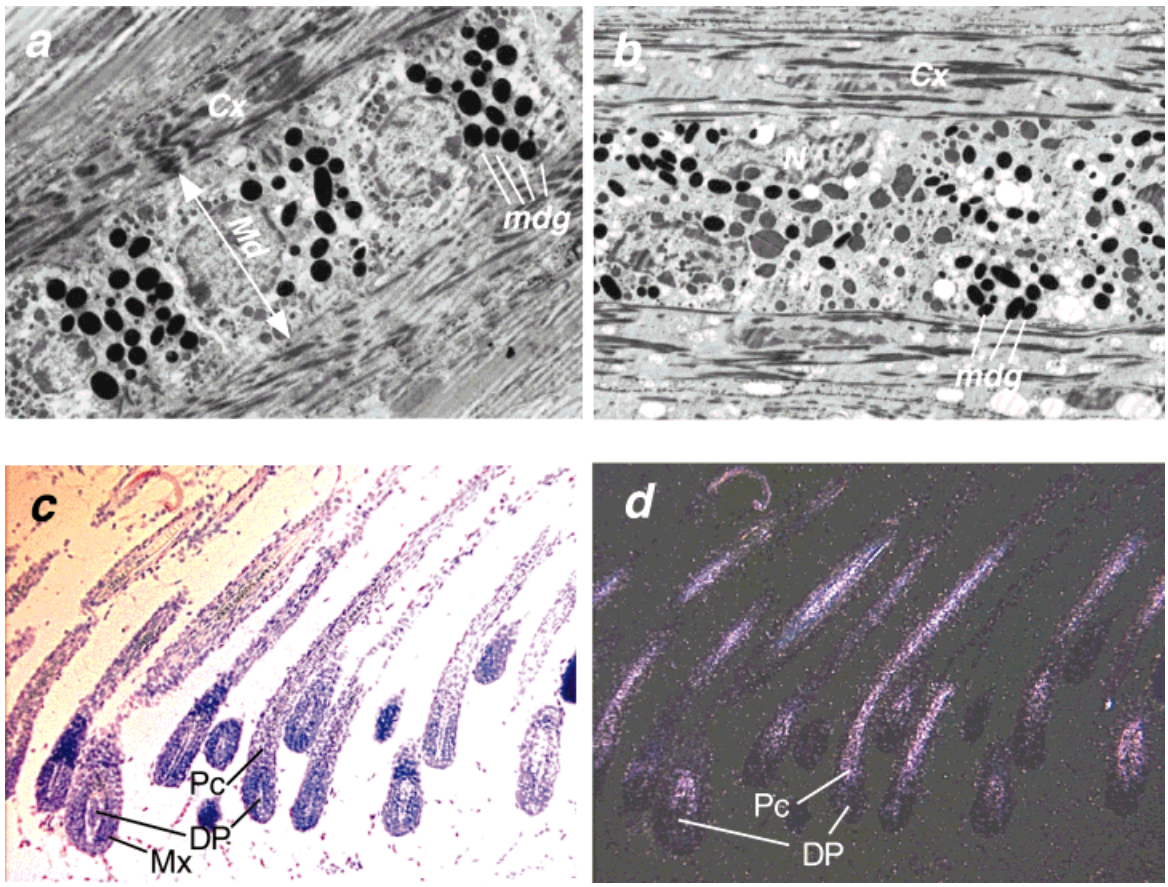

FIG. 5. Transmission electron microscopy (3,200×) of pelage hair (*a, b*). Longitudinal sections of the dorsal skins from mice on P11: (**a**) wild-type, +/+; (**b**) ENU-induced satin, sa^{e1}/sa^{e1}. Expression of *Foxq1* in dorsal skin of a 9-day-old mouse (**c, d**). *Foxq1* is expressed only in precursor cells of the hair shaft medulla. Bright field (c) and corresponding dark field (d) images are shown for in situ hybridizations using ^{35}S-labeled riboprobes. Cx = cortex layer; DP = dermal papilla; N = nucleus; Md = medullary layer; mdg = medullary dense granule; Mx = matrix cells; Pc = precursors of hair shaft.

tion from the thymus and spleen. Lymphocyte supopulations were assessed by flow cytometry and serum immunoglobins were also measured. In addition, we examined T-cell and B-cell function in vitro by measuring their proliferation in response to polyclonal mitogens, such as concanavalin A (ConA) or lipopolysaccharide (LPS), which preferentially activates T and B cells, respectively. First, we compared homozygous 5–week-old satin animals for the ENU allele (sa^{e1}/sa^{e1}) with age–matched wild-type progenitor C3H inbred mice to show some reduction in the number of lymphocyte subpopulations in satin (Fig. 6). However, all subsequent evaluations of the heterozygote and wild-type littermates (+/+, $+/sa^{e1}$) of the ENU-induced satin allele failed to detect any significant differences compared to the homozygote satin mice (sa^{e1}/sa^{e1}), indicating that *Foxq1* is unlikely to be critically involved in the T- and B-cell development or differentiation. Furthermore, histological sections of the thymus and spleen showed no apparent structural defects in satin mice (data not shown). Thus, immune defects in satin mice, originally observed by McGarry *et al.* (1984), is likely attributable to the 3H1 (C3H × 101 hybrid strain) genetic background. It is possible that *Foxq1* may have a minor effect in the maintenance of the immune system, and thus comprehensive functional analysis of the lymphocytes may be useful.

Hair growth requires a delicate balance of a complex signaling and inductive interaction between dermal and epidermal cells, which engages in cycles of growth and regression throughout adult life. The molecular mechanisms controlling hair formation, however, remain largely unidentified. We report here that a winged helix (WH)/forkhead transcription factor, *Foxq1*, acts uniquely on the matrix cells of the follicle that subsequently give rise to the medullary cells. The hair phenotype in satin mice must arise from the failure of *Foxq1* to activate or repress a downstream factor required for normal hair development, especially in development of the medullary cells. Abnormalities in the hair shaft medulla could arise from a number of defects: 1) a defect in cell lineage (failure of matrix cells to give rise to premedullary cells), 2) a defect in differentiation (absence of medullary cell-specific proteins), or 3) a defect in cell-cell communication

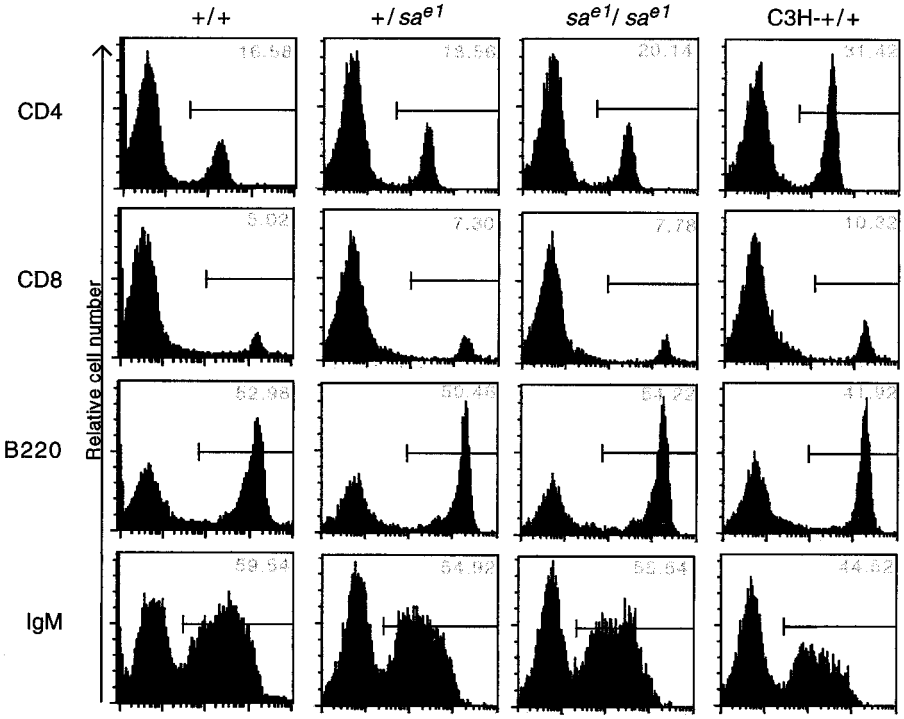

FIG. 6. FACS analysis of spleen cells from 5-week-old mice. T and B cells of homozygous satin mutants of the ENU allele (sa^{e1}/sa^{e1}) (n = 5) was compared to its heterozygous ($+/sa^{e1}$) (n = 3) and wild-type (+/+) littermates (n = 4), and wild-type C3H inbred mice (n = 2). The CD4 and CD8 coreceptor proteins distinguish the major T-cell subsets. The percentage of cells positive for a given marker is indicated. There are no significant differences in the lymphocyte subpopulation in any of the genotypes (+/+, $+/ sa^{e1}$, sa^{e1}/sa^{e1}) from the strain in which the ENU-induced allele is maintained. However, strain-specific differences were observed when compared to the wild-type C3H inbred mice. Similar results were attained for the B-cell surface markers B220 and IgM. FACs analysis of thymus cells was also performed using the CD4, CD8, and Thy-1 coreceptor proteins with similar results observed.

(failure of cortical cells to produce signals required for proper maintenance of medullary cell function). Although further high-resolution studies will be necessary to identify the specific nature of the medullary defects, our preliminary expression and ultrastructural examinations suggest that hair defects in satin mice are cell autonomous, failure in differentiation of the medulla, and also likely the cortex.

Recent data have shown that the *Delta-Notch* signaling pathway and the WNT pathway are key components in the formation of the hair follicle and in differentiation of the hair shaft (Powell *et al.*, 1998; Millar *et al.*, 1999; Lin *et al.*, 2000). Interestingly, transgenic mice overexpressing Notch exhibit a sheen appearance similar to that of satin mice, in addition to hair loss caused by the changes in the bulb ends of hair (Lin *et al.*, 2000). Their medullary cells lacked air spaces, altering the refractive properties of the coat, as seen in satin mice. In these trangenic lines, the Notch target is never detected in the medulla; Notch is normally expressed in matrix cells and in precursor cells of the cortex, cuticle, and inner root sheath. Therefore, it has been suggested that ectopic expression of Notch in the cortex results in abnormal differentiation of the neighboring medulla and cuticle through cell-cell interaction (Lin *et al.*, 2000). It is especially interesting that activated expression of Notch give rise to abnormalities very similar to those in satin hairs. It remains to be determined whether Notch activity in the cortex affects the *Foxq1* signaling pathway.

METHODS

Mice

Doubly homozygous beige-satin mice (SB/Le-*bg sa* / *bg sa*), C3HeB/FeJ and DNA from homozygous wild-type SB/Le mice (SB/Le-++/++) were obtained from The Jackson Laboratory (Bar Harbor, ME); the wild-type livestock (SB/Le-++/++) is no longer available.

ENU Mutagenesis and Screening

Homozygous satin females (SB/Le-*bg sa* / *bg sa*) were crossed with ENU-treated (101 × C3H)F_1 males, allowing the recovery of additional satin and beige alleles among the offspring based on their hair color and sheen. The ENU treatment consisted of 4 weekly fractionated injections at 85 mg/kg body weight for a total dose of 340 mg/kg. A total of 347 F_1 mice were screened; one allele of satin (sa^{e1}) and two alleles of beige were recovered. Each of these mutations was shown to be heritable in subsequent crosses.

Genomic Analysis of Mouse *Foxq1*

PCR reactions were carried out as previously described (Hong *et al.*, 1999). Samples were processed through an initial denaturation (96°C for 4 min), followed by 35 cycles of denaturation (94°C, 30 s), annealing (55°C, 30 s), elongation (72°C, 30 s), and terminated by a 10-min elongation at 72°C. The radiation-induced satin allele (67 bp deletion) was detected using the primers m*Foxq1*.F2 (5′- GAGATCAACGAGTACCTCATGGG-3′) and m*Foxq1*.R5 (5′-CGAAGGAGCTGGAGAACTTG-3′); the ENU-induced satin allele

was detected using the primers mHhf1.F3 (5′-GGCAACTGATGACAGCAGAA-3′) and m*Foxq1*.R4 (5′-TGACGAAACAGTCGTTGAGC-3′) followed by *Fok1* (NEB, Beverly, MA) restriction enzyme digestion. Amplified products were separated on 2.0–2.5% agarose gels. The full-length *Foxq1* gene was amplified using the primers 5′-TTCGGAAAAGCGTCTCTCTCGGA-3′ and 5′-TTAGCACATTTGATGGAGAGTTG-3′. Amplification products were directly sequenced or subcloned into pCR2.1 using the Original TA cloning kit (Invitrogen, Carlsbad, CA). Nucleotide sequencing was performed using the ABI PRISM™ Dye Terminator Cycle Sequencing Ready Reaction Kit (Perkin Elmer, Foxter City, CA) and sequences were aligned using a Multiple Alignment algorithm (http://www.genebee.msu.su/services/malign_reduced.html; Belozersky Institute, Moscow State University, Moscow, Russia).

Expression Analysis of *Foxq1*

Mouse embryo and total mouse multiple tissue northern blots (MTN™; Clontech, Palo Alto, CA) were hybridized at 68°C, washed to a final stringency of 0.1 × SSC, 0.1% SDS at 55°C (40 min), and exposed to autoradiography using probes labeled with [α-^{32}P]dCTP. Membranes were first probed with a 706 bp mouse *Foxq1* fragment (amino acids 272–400 from the initiation methionine codon plus 316 bp of the 3′ UTR) and then a 776 bp mouse *Foxq1* fragment from the 5′ end (excluding the WH DNA-binding domain). The 776 bp fragment consists of 517 bp of the 5′ UTR plus the first 86 amino acids. Blots were washed in sterile 0.5% SDS at 90–100°C for 15 min and exposed to X-ray film to confirm removal of the probe between hybridizations. Total RNA was isolated from dissected mouse adult tissues using the guanidinium/cesium chloride method (Sambrook *et al.*, 1989). RNA was denatured, size-fractionated by electrophoresis on formaldehyde agarose gels, capillary-blotted to nylon membranes (Sambrook *et al.*, 1989), and hybridized as described. As a control for RNA integrity, membranes were hybridized with a mouse-*actin* probe. In situ hybridization to sectioned tissue was performed as described (Angerer and Angerer, 1992). A 706 bp mouse *Foxq1* fragment was used to prepare an [^{35}S-]-UTP-labeled antisense riboprobe.

Flow Cytometry and In Vitro Proliferation Assay

Single cell suspensions of the spleen and thymus were prepared from 5-week-old sex-matched satin mutants (sa^{e1}/sa^{e1}) and their littermates ($+/sa^{e1}$, +/+). Two mice of each genotype were analyzed. Cells were washed (PBS supplemented with 0.5% newborn calf serum, 0.01% NaN_3, pH7.4) and blocked with normal mouse serum (5%) on ice for 25–30 min. Cells were then incubated with PE conjugated irrelevant control antibody, and anti-CD4, anti-CD8, anti-Thy-1, anti-B220, or anti-sIgM (Pharmingen, CA). Samples were washed and fixed with 1% paraformaldehyde. Stained and fixed cells were analyzed in a FACScan (Becton Dickinson, CA); at least 5,000 cells were analyzed per sample in all experiments. For in vitro proliferation assays, a single cell suspension was prepared from spleens and cultured at 2.5×10^5 cells/well with different doses of ConA or LPS , which preferentially activate T cells and B cells, respectively. Cells were incubated for 48 h at 37°C in 5% CO_2 and saturated humidity, and then pulsed for an additional 16 h with 1 μCi of [^{3}H]-thymidine. Cells were harvested with a PHD cell harvester (Cambridge, MA) and counts (cpm) obtained from a scintillation counter.

Capture ELISA Analysis

A 96-well plate was coated with goat anti-mouse Ig capture antibody (5–10 μg/ml; Southern Biotech Assoc., Birmingham, AL) for a minimum of 12 h at 4°C and then washed and blocked with BSA (1%) for 1 h at room temperature. Diluted serum (1:500, 1:5000) was added and incubated for 2–3 h. After washing, AP conjugated anti-Ig, anti-IgA, anti-IgM, anti-IgG1, anti-IgG2a, anti–IgG2b, or anti–IgG3 (Southern Biotech Assoc., Birmingham, AL) was added and incubated for 1 h at room temperature. Optical density was read at 405 nm at 10 min and 20 min after addition of p-nitrophenyl phosphate substrate (1 mg/ml; Southern Biotech Assoc., Birmingham, AL).

Isolation and Mapping of Human *FOXQ1*

Two human bacterial artificial chromosome clones (447e13 and 555c10) were identified from a human BAC library (RPCI11 Human BAC Library, Roswell Park, NY) by high-stringency hybridization screening using a 366 bp human *FOXQ1* probe generated by the primers 5′-GAGATCAACGAGTACCTCATGGG-3′ and 5′-CAAGTTCTCCAGCTCCTTCG-3′ from genomic DNA. Because the WH DNA-binding domains of rodent and human *FOXQ1* are highly conserved, a human-specific fragment (cwrH555) common to both BAC clones was isolated using the IRS-PCR method (Nelson *et al.*, 1989). The fragment cwrH555 was mapped to human chromosome 6p25 in proximity to the marker SHGC-33618 (lod score, 4.22; map distance, 52.98 cR) using the Stanford G3 Radiation Hybrid Mapping Panel (Stewart *et al.*, 1997) (Research Genetics, Huntsville, AL). The data were analyzed using the Stanford RH Web Server (http://wwwshgc.stanford. edu/RH/index.html). PCR amplification of the cwrH555 fragment was performed using the primers 5′-CCGTGGTTCTAGAAAGCGAT-3′ and 5′-TGCCTTCAAAGGGAAGAAAA-3′.

EMBL/GenBank Accession Numbers

Mouse *Foxq1* gene, AF154426; human *FOXQ1* gene, AF153341; rat *Foxq1* gene, AF153193; rat *Foxq1* cDNA, L13201; mouse *Foxa1(HNF-3α)*, *X74936; Foxa2-(HNF-3β)*, X74937; mouse *Foxa3 (HNF-3γ)*, X74938; mouse *Foxq1 (Hfh-1L),* AF010405.

ACKNOWLEDGMENTS

We thank Drs. Ron Conlon, Karl Herrup, Terry Magnuson, and Ray Redline for many helpful discussions; Dr. Evan Eichler for providing rat genomic DNA; Dr. Jose Marcelino for technical advice; and Kim Bentley, Don

Carpenter, and Nydia Bringht-Twumasi for technical assistance. This work was supported by NIH grant HD 34857 to A.C. and a grant from the Willson Foundation to the Center for Human Genetics.

LITERATURE CITED

Angerer LM, Angerer RC. 1992. In situ hybridization to cellular RNA with radiolabelled RNA probes. In: Wilkinson DG, editor. In situ hybridization: a practical approach. Oxford: IRL Press. p 15–32.

Clark KL, Halay ED, Lai E, Burley SK. 1993. Co-crystal structure of the HNF-3/forkhead DNA-recognition motif resembles histone H5. Nature 364:412–420.

Clevidence DE, Overdier DG, Tao W, Qian X, Pani L, Lai E, Costa RH. 1993. Identification of nine tissue-specific transcription factors of the hepatocyte nuclear factor3/forkhead DNA-binding-domain family. Proc Natl Acad Sci U S A 90:3948–3952.

Clevidence DE, Overdier DG, Peterson RS, Porcella A, Ye H, Paulson KE, Costa RH. 1994. Members of the HNF-3/forkhead family of transcription factors exhibit distinct cellular expression patterns in lung and regulate the surfactant protein B promoter. Dev Biol 166:195–209.

Frank J, Pignata C, Panteleyev AA, Prowse DM, Baden H, Weiner L, Gaetaniello L, Ahmad W, Pozzi N, Cserhalmi-Freidman PB, Aita VM, Uyttendaele H, Gordon D, Ott J, Brissette JL, Christiano AM. 1999. Exposing the human nude phenotype. Nature 398:473–474.

Frank S, Zoll B. 1998. Mouse HNF-3/fork head homologue-1 like gene: structure, chromosomal localization and expression in adult and embryonic kidney. DNA Cell Biol 17:679–688.

Hardy MH. 1992. The secret life of the hair follicle. Trends Genet 8:55–61.

Hong H-K, Lass J H, Chakravarti A. 1999. Pleiotropic skeletal and ocular phenotypes of the mouse mutation congenital hydrocephalus (*ch/Mf1*) arise from a hepatocyte nuclear factor 3/forkhead winged helix transcription factor gene. Hum Mol Genet 8:625–637.

Kaestner K, Knöchel W, Martínez D. 2000. Unified nomenclature for the winged helix/forkhead transcription factors. Genes Dev 14: 142–146.

Kaufmann E, Knöchel W. 1996. Five years on the wings of forkhead. Mech Dev 57:3–20.

Lin M-H, Leimeister C, Gessler M, Kopan R. 2000. Activation of the Notch pathway in the hair cortex leads to aberrant differentiation of the adjacent hair-shaft layers. Development 127:2421–2432.

Major MH. 1955. Satin, *sa*. Mouse News Letter 12:47.

McGarry RC, Walker R, Roder JC. 1984. The cooperative effect of the satin and beige mutations in the suppression of NK and CTL activities in mice. Immunogenetics 20:527–534.

Millar SE, Willert K, Salinas PC, Roelink H, Nusse R, Sussman DJ, Barsh GS. 1999. WNT signaling in the control of hair growth and structure. Dev Biol 207:133–149.

Mitchell PJ, Tjian R. 1989. Transcriptional regulation in mammalian cells by sequence-specific DNA binding proteins. Science 245: 371–378.

Nehls M, Pfeifer D, Schorpp M, Hendrich H, Boehm T. 1994 New member of the winged-helix protein family disrupted in mouse and rat nude mutations. Nature 372:103–107.

Oro AE, Scott MP. 1998. Splitting hairs: Dissecting roles of signaling systems in epidermal development. Cell 95:575–578 .

Nelson DL, Ledbetter SA, Corbo L, Victoria MF, Ramierz-Solis R, Webster TD. Ledbetter DH, Caskey CT. 1989. Alu polymerase chain reaction: a method for rapid isolation of human-specific sequences from complex DNA sources. Proc Natl Acad Sci U S A 86:6686–6690.

Parakkal PF. 1969. The fine structure of anagen hair follicle of the mouse. Adv Biol Skin 9:441–469.

Perou, CM, Perchellet A, Jago T, Pryor R, Kaplan J, Justice MJ. 1997. Comparative mapping in the *beige-satin* region of mouse chromosome 13. Genomics 39:136–146.

Powell BC, Passmore EA, Nesci A, Dunn SM. 1998. The Notch signalling pathway in hair growth. Mech Dev 78:189–192.

Qian X, Costa RH. 1995. Analysis of hepatocyte nuclear factor 3-protein domains required for transcriptional activation and nuclear targeting. Nucl Acid Res 23:1184–1191.

Rinchik EM. 1991 Chemical mutagenesis and fine-structure functional analysis of the mouse genome. Trends Genet 7:15–21.

Sambrook J, Fritsch EF, Maniatis T. 1989. Molecular cloning: a laboratory manual. Cold Spring Harbor, NY: Cold Spring Harbor Laboratory.

Schüddekopf K, Schorpp M, Boehm T. 1996. The whn transcription factor encoded by the nude locus contains an evolutionarily conserved and functionally indispensable activation domain. Proc Natl Acad Sci U S A 93:9661–9664 .

Spritz RA. 1998. Genetic defects in Chediak-Higashi syndrome and the beige mouse. J Clin Immun 18:97–105.

van Steensel MAM, Happle R, Steijlen PM. 2000. Molecular genetics of the hair follicle: the state of the art. PSEBM 223:1–7.

Stewart EA, McKusick KB, Aggarwal A, Bajorek E, Brady S, Chu A, Fang N, Hadley D, Harris M, Hussain S, Lee R, Maratukulam A, O'Connor K, Perkins S, Piercy M, Qin F, Reif T, Sanders C, She X, Sun W-L, Tabar P, Voyticky S, Cowles S, Fan J-B, Mader C, Quackenbush J, Myers RM, Cox DR. 1997. An STS-based radiation hybrid map of the human genome. Genome Res 7:422–433.

Sundberg JP, King Jr LE. 1996. Mouse mutations as animal models and biomedical tools for dermatological research. J Invest Dermatol 106:368–376.

Trigg MJ. 1972. Hair growth in mouse mutants affecting coat texture. J Zool (Lond) 168:165–198.